Proc. Natl. Acad. Sci. USA
Vol. 82, pp. 1604–1608, March 1985
Biochemistry

The NADPH binding site on beef liver catalase

(catalase structure/bound NADPH/mammalian and fungal comparison)

IGNACIO FITA AND MICHAEL G. ROSSMANN

Department of Biological Sciences, Purdue University, West Lafayette, IN 47907

Contributed by Michael G. Rossmann, November 1, 1984

ABSTRACT **Beef liver and human erythrocyte catalases (EC 1.11.1.6) bind NADP tenaciously [Kirkman, H. N. & Gaetani, G. F. (1984) *Proc. Natl. Acad. Sci. USA* 81, 4343–4348]. The position of NADP on beef liver catalase corresponds to the carboxyl-terminal polypeptide hinge in *Penicillium vitale* fungal catalase, which connects the common catalase structure to the additional flavodoxin-like domain. In contrast to nearly all other known structures of protein-bound NADP, NAD, and FAD, the NADP molecule of beef liver catalase is folded into a right-handed helix and bound, in part, in the vicinity of the carboxyl end of two α-helices. A water molecule (W7) occupies a pseudosubstrate site close to the C4 position of the nicotinamide and is hydrogen bonded to His-304. Although the NADP and heme groups approach each other to within 13.7 Å, there is no direct interaction. The function of the NADP remains a mystery.**

Kirkman and Gaetani (1) have recently shown that tetrameric human and beef catalase (hydrogen-peroxide:hydrogen-peroxide oxidoreductase, EC 1.11.1.6) binds four molecules of NADPH with a dissociation constant less than 1×10^{-8} M. While they make some suggestions as to the function of the bound dinucleotide, there is yet no true understanding of its physiological significance. Although the NADP can be removed only by a series of partially denaturing agents, it does not seem to be involved in the catalatic or peroxidatic activity.

The crystal structure of beef liver catalase (BLC) has been determined (2, 3) and more recently refined (unpublished results). The crystal structure of the fungal (*Penicillium vitale*) catalase (PVC) has also been determined (ref. 4; unpublished results) and was seen to be very similar to BLC apart from an additional carboxyl-terminal domain that has a flavodoxin-like structure. The "hinge" polypeptide, between the common catalase structure and the flavodoxin domain, binds into an external cleft of the molecule.

A significant volume of uninterpreted density occurred in the refined BLC electron density map at the equivalent position occupied by the hinge in PVC. This had tentatively been interpreted in terms of a carboxyl-terminal extension of BLC, consistent with the occasional occurrence of peptides in the digested protein (5). These peptides were homologous to a carboxyl-terminal extension of beef erythrocyte catalase (Table 1). However, when it was suggested (1) that NADP is bound to catalase, then the interpretation of the extra density as NADP was immediately obvious (Fig. 1). Its approximate position on the enzyme surface, corresponding to the hinge region leading to the flavodoxin domain of PVC, is shown in Fig. 2. The model of NADP was subsequently refined with respect to the observed structure amplitudes, giving an overall final *R* factor of 19.1% for 33,255 reflections extending to 2.5-Å resolution. The coordinates of the NADP prosthetic group are given in Table 2 and are also deposited with the Brookhaven Protein Data Bank.

Table 1. Erroneous carboxyl-terminal sequence extension of BLC by alignment with bovine erythrocyte catalase (BEC)

Catalase	Sequence
BLC [Schroeder *et al.* (5)]	500 505 515 -N-E-E-K-P-K-N(V,E,H,G,S,H)(V-H-T-Y) Th10 Th11
BLC (x-ray)	-N not visible H- V-H-T-Y-A
BEC [Schroeder *et al.* (5)]	-N-E-E-K-P-K-N(V-E-H-G-S-H)(V-H-T-Y,A)
PVC [Vainshtein *et al.* (4), x-ray]	495 500 505 -A - A-A-A-A-A-A-A-A-A-A- A-A-A-A-A

The peptides Th10 and Th11 occurred only in occasional isolates of BLC. The position of the extra density of BLC had been erroneously interpreted as the peptide H-V-H-T-Y-A in a position corresponding to the hinge between the common catalase structure and the flavodoxin-like domain in PVC.

Conformation of NADP when bound to catalase

It has been proposed (6, 7), on the basis of NMR studies, that at neutral pH and room temperature, NAD^+ exists in equilibrium between two folded forms and an extended form (Fig. 3). The folded forms make either left- or right-handed helices and are considered to be of lower energy than the extended form. Nevertheless, the structures of NAD [lactate dehydrogenase (9, 10), alcohol dehydrogenase (11, 12), malate dehydrogenase (13), glyceraldehyde-3-phosphate dehydrogenase (14, 15), L-3-hydroxyacyl-coenzyme A dehydrogenase (16), phosphorylase (2 sites) (17), and sorbitol dehydrogenase (18)], NADP [dihydrofolate reductase (19), glutathione reductase (20), *p*-hydroxybenzoate hydroxylase (by comparison with glutathione reductase) (21, 22), and 6-phosphogluconate dehydrogenase (23, 24)] and FAD [glutathione reductase (25) and *p*-hydroxybenzoate hydroxylase (26)] (reduced or oxidized) have an extended conformation (base separation of at least 14 Å) when bound to enzyme in nearly all cases. The overall conformations of the bound dinucleotides are all very similar (cf. ref. 27). The only exception is that of sorbitol dehydrogenase, for which an NMR study (18) produces the paradoxical result that the base separation is merely 8.5 Å, although the enzyme is homologous to liver alcohol dehydrogenase.

Free NAD^+ has been crystallized as a lithium salt (28) and as a free acid (29). The conformation of the dinucleotide in these two crystal structures differs greatly from the common conformation found when bound to enzymes. Indeed, the free acid NAD^+ structure is partially folded, with the minimum distance between bases of only 9.6 Å.

When dinucleotides are bound to enzymes, they are al-

The publication costs of this article were defrayed in part by page charge payment. This article must therefore be hereby marked "*advertisement*" in accordance with 18 U.S.C. §1734 solely to indicate this fact.

Abbreviations: BLC, beef liver catalase; PVC, *Penicillium vitale* catalase; DHFR, dihydrofolate reductase.

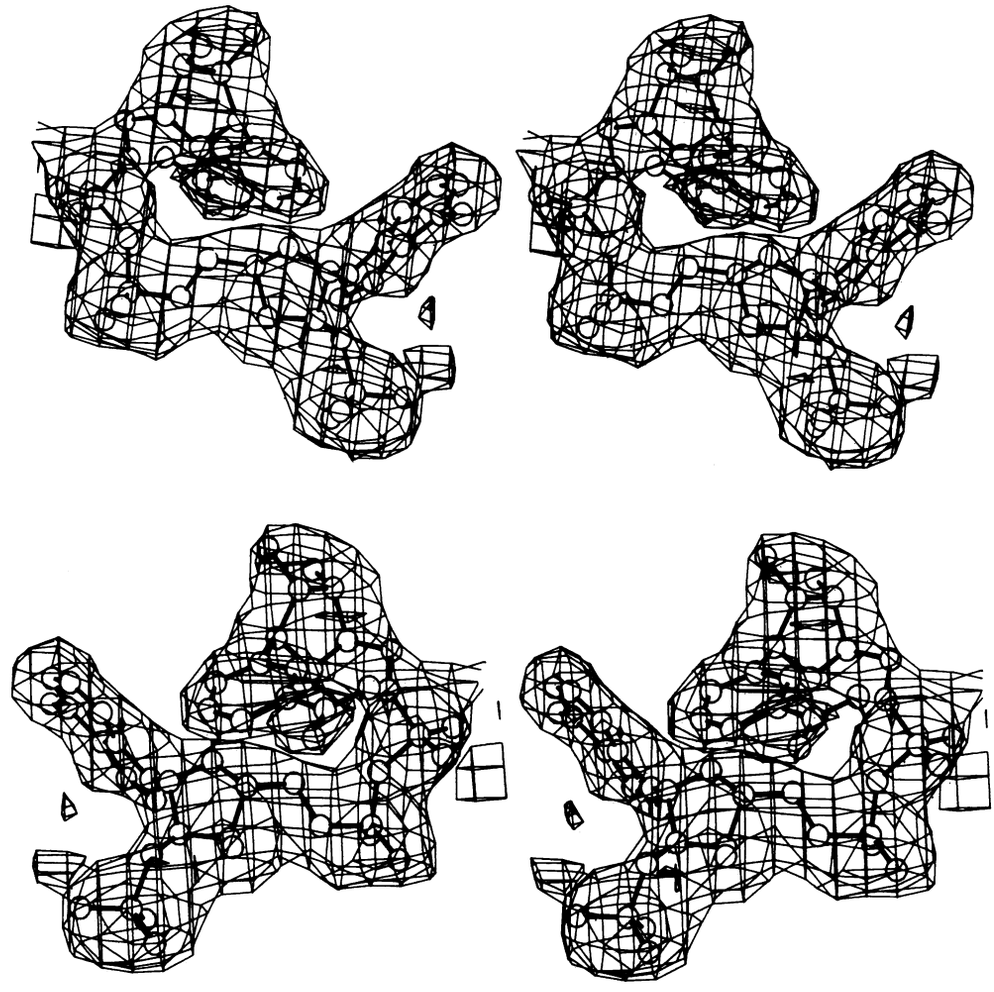

FIG. 1. Two stereo views of the "extra density" in an electron density map of BLC, in which the two crystallographically independent subunits had been averaged. The structure of NADP is superimposed. The BLC map is dependent on phases calculated from the refined molecule (R = 19.1%) for which the extra density had been erroneously interpreted as a H-V-H-T-Y-A peptide (Table 1). Nevertheless, the fit to NADP is excellent and far superior to the erroneous peptide assumption.

most invariably associated with an α/β structure (a "nucleotide-binding" fold). The cofactor is then bound to the carboxyl end of strands in a parallel β-pleated sheet and to the amino end of parallel α-helices. The structural significance of this fold is probably due to the electrostatic dipole moment exerted by the α-helices on the negatively charged phosphates (30). The structure itself may be the result of divergent evolution from a primordial mononucleotide-binding fold (31, 32) or convergent evolution to a stable supersecondary structure (33). The only exception is that of 6-phospho-

Table 2. Coordinates of the NADP molecule bound to BLC

Atom	P, Å	Q, Å	R, Å	Atom	P, Å	Q, Å	R, Å	Atom	P, Å	Q, Å	R, Å
N1A	24.1	6.6	34.3	OP3	26.7	14.9	32.4	O1'N	31.7	7.5	31.9
C2A	24.6	7.2	33.1	C3'A	29.0	11.9	32.8	C4'N	32.8	6.6	32.1
N3A	25.5	8.1	33.0	O3'A	29.0	12.6	31.3	C3'N	32.4	5.2	31.6
C4A	26.0	8.6	34.2	C4'A	29.6	10.5	32.6	O3'N	31.9	4.3	32.5
C5A	25.6	8.2	35.5	O1'A	28.7	9.6	33.2	C2'N	31.3	5.6	30.6
C6A	24.6	7.1	35.5	C5'A	31.0	10.3	33.1	O2'N	30.5	4.5	30.4
N7A	26.3	9.0	36.5	O5'A	31.7	11.6	33.0	C1'N	30.6	6.7	31.3
C8A	27.1	9.9	35.8	PA	33.2	11.6	33.3	N1N	30.1	7.7	30.6
N9A	26.9	9.6	34.5	OP1A	33.3	11.4	34.7	C2N	31.0	8.2	29.7
N6A	24.1	6.6	36.6	OP2A	33.9	12.8	32.7	C3N	30.6	9.3	28.9
C1'A	27.4	10.1	33.3	O	33.5	10.2	32.6	C4N	29.3	9.8	29.0
C2'A	27.6	11.6	33.1	PN	34.6	9.5	31.7	C5N	28.5	9.2	29.9
O2'A	26.8	12.4	32.4	OP1N	35.7	9.1	32.5	C6N	28.8	8.1	30.7
P	26.2	13.7	33.2	OP2N	35.1	10.5	30.6	C7N	31.5	10.0	27.8
OP1	26.6	13.7	34.6	O5'N	33.7	8.4	31.0	N7N	32.8	9.5	27.7
OP2	24.7	13.6	33.2	C5'N	34.0	7.1	31.5	O7N	31.1	10.9	27.2

Coordinates are given with respect to the P, Q, R molecular diad axes (3) for the "standard" subunit. In the designations of the atoms, an A as the last character refers to adenine; an N, nicotinamide.

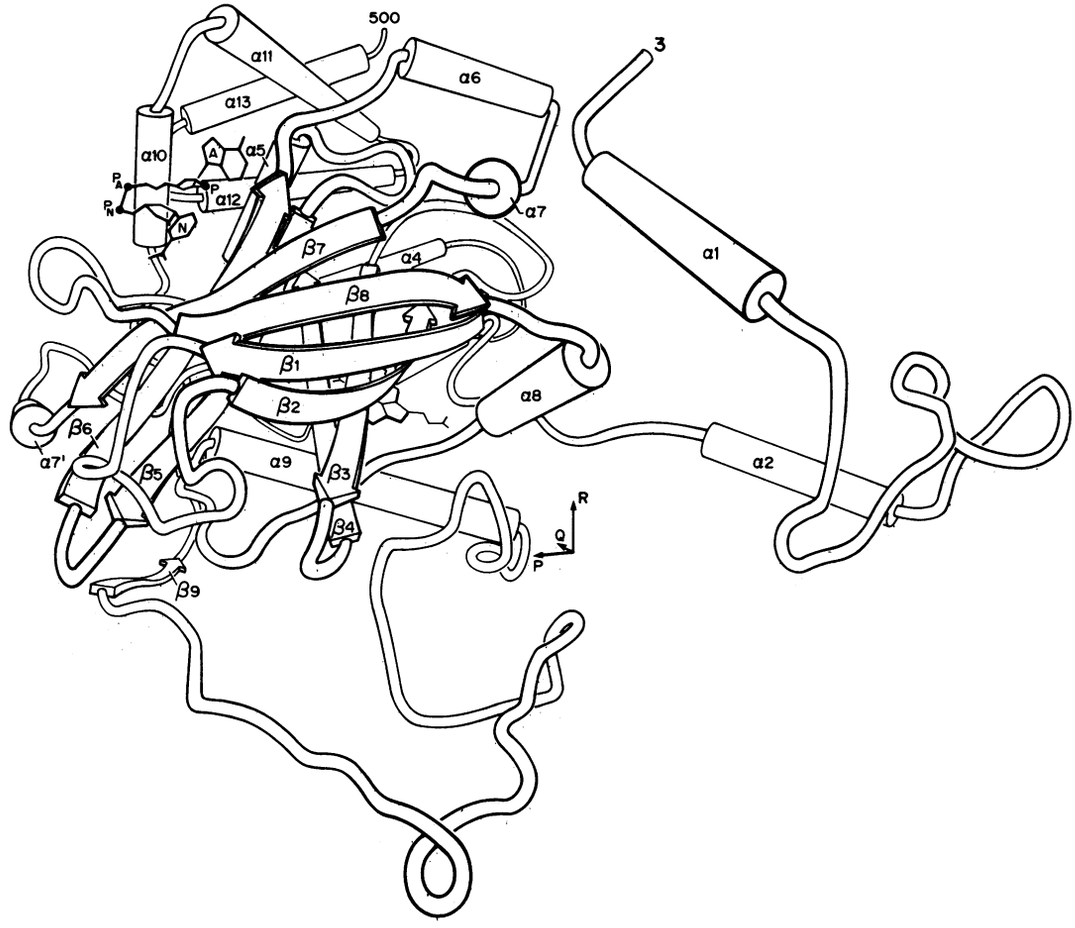

FIG. 2. Diagrammatic view of one subunit of BLC, showing the position of the bound NADP molecule on the enzyme. A C_α backbone diagram that includes a view of the bound NADP and heme groups will be published elsewhere.

gluconate dehydrogenase, which is predominantly an α structure, with the possibly extended NADP coenzyme apparently binding in the proximity of the carboxyl end of helices VIb and XII (23).

NADP bound to catalase is not extended but rather is folded into a right-handed helix, although the bases are approximately perpendicular rather than parallel (Fig. 1). The nicotinamide ring is roughly parallel to the adenine ribose, with a closest approach of 3.6 Å. The binding site on the protein is toward the carboxyl ends of helices α5 and α10 (Fig. 2). The bases are close to these two helices, while the phosphates are furthest away from them.

The conformational angles [cf. ref. 9 for their definition; in addition, the dihedral angle θ'_a relates to the C2'(a)—O2'(a) bond giving the position of the O2' bound phosphate] of the coenzyme are shown in Table 3, where they are compared with the well-refined extended NADP structure found in *Lactobacillus casei* dihydrofolate reductase (DHFR) (19) as well as with the tentative, low-resolution, structure of NADP in 6-phosphogluconate dehydrogenase (24). The adenosine nucleoside structures of NADP bound to BLC and to DHFR are very similar, with the O2' phosphate positioned in the sterically favored *trans* orientation relative to the ribose ring. The puckering of the adenosine ribose ring in BLC·NADP is not clear since the C1'—C2'—C3'—C4' dihedral angle ψ is only 5°. The nicotinamide mononucleoside structures in NADP of BLC and DHFR are also similar except that BLC·NADP is *syn* at the glycosidic bond, whereas the DHFR·NADP structure is *anti*. The puckering of the nicotinamide ribose ring in DHFR·NADP is given by $\psi = -36°$ (C2' endo). The major differences in these two NADP structures are the conformational angles of the pyrophosphate groups, producing a folded conformation in one case and extended in the other. Thus viewing down the P_a–P_n line shows the 5' oxygens nearly *cis* to each other in BLC·NADP and nearly *trans* in DHFR·NADP. The orientation of the carboxyamide group, while clearly planar with the nicotinamide ring, can be determined only tentatively by consideration of the hydrogen bonding environment. For BLC·NADP, the N7 position has been assigned *trans* to N4 of the nicotinamide. The orientation of this group in small molecule structures is *trans* for the NAD Li salt (28) and *cis* in the NAD free acid (29) and in a structure of nicotinamide (35).

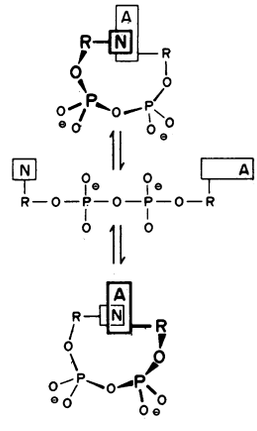

FIG. 3. Folded and extended forms of NAD^+ in aqueous solution [adapted from Saenger *et al.* (8)].

Table 3. Conformations of NADP and NAD molecules

Angle	Defining atoms	Dihedral angle, ° NADP catalase	NADP in *L. casei* DHFR*	NADP in 6PDH†	NAD of LDH·NAD·pyruvate in M_4 LDH‡
χ_a	C4(A), N9(A), C1'(A), C2'(A)	139	105	100	89
Ribose a conformation		C2' endo?	C3' endo	?	C3' endo
θ'_a	C1'(A), C2'(A), O2'(A), P	125	145	−102	
ξ_a	C3'(A), C4'(A), C5'(A), O5'(A)	−25	−169	−169	−78
θ_a	C4'(A), C5'(A), O5'(A), P(A)	−173	−163	−134	−159
ψ_a	C5'(A), O5'(A), P(A), O	37	−72	110	109
ϕ_a	O5'(A), P(A), O, P(N)	144	141	−156	−156
ϕ_n	O5'(N), P(N), O, P(A)	−161	82	−160	49
ψ_n	C5'(N), O5'(N), P(N), O	−109	57	109	87
θ_n	C4'(N), C5'(N), O5'(N), P(N)	118	129	180	−171
ξ_n	C3'(N), C4'(N), C5'(N), O5'(N)	−54	−172	−88	−53
Ribose n conformation		C2' endo	C2' endo	?	C3' endo
χ_n	C2(N), N1(N), C1'(N), C2'(N)	−54	117	−81	106
Shortest distance between adenine and nicotinamide		3.9 Å [C6(A)–N3(N)]	12 Å [C8(A)–C6(N)]	14 Å	14.0 Å [C6(A)–C2(N)]
α	N9(A), P(A), P(N), N1(N)		170	?	58

The convention for the dihedral angle nomenclature is that of Arnott and Hukins (34). The angles are positive for right-handed rotations (that is, the far end of any bond is rotated clockwise relative to the near end). The zero angle of rotation is the *cis* conformation for successive bonds in the chain.
*Filman *et al.* (19).
†Data for 6-phosphogluconate dehydrogenase from Abdallah *et al.* (24).
‡Data for lactate dehydrogenase from Chandrasekhar *et al.* (9).

Environment of NADP in BLC

A stereo view of the interacting residues and water molecules is shown in Fig. 4 and described in Table 4. The adenine moiety binds to a hydrophobic surface, as is usual in other NAD and NADP binding proteins. The O2' phosphate interacts with Arg-202, Asp-212, and Lys-236. Indeed, it had been noted by Murthy *et al.* (3) that Lys-236 had no apparent charge balance. This situation has now been resolved by the interpretation of the extra density as NADP. The pyrophosphate group interacts with His-304, which also interacts with the C4 position of the nicotinamide and the "substrate" water W7. There is extensive electron density between the adenine phosphate and His-304. This might represent a strong interaction (the distance between the phosphate oxygen and the imidazole nitrogen is 2.5 Å) and relate to the dissociation constant of less than 10^{-8} M (1). In contrast, the pyrophosphate moiety of many NAD-dependent dehydrogenases interacts with arginine residues (cf. ref. 14). Both OH groups of the nicotinamide ribose form hydrogen bonds with the protein. The orientation of the nicotinamide is fixed primarily by hydrogen bonding interactions with the carboxyamide group.

The interaction of Lys-236 and Arg-202 with the O2' phosphate of NADP explains why NADP binds better than NAD (1) and why the uncharged reduced cofactors bind better than the charged oxidized cofactors. The position of the dinucleotide in the cleft occupied by the hinge region in PVC also suggests why NADP does not bind as well to human erythrocyte catalase as to BLC. The former has a carboxyl-terminal extension (Table 1) that is likely to compete for the binding of NADP in the same cleft.

Of particular interest is the water molecule W7, which is positioned about 4 Å from the reactive C4 position of the nicotinamide relative to the A side (pro-*R*) of the ring. Furthermore, this water is within 3.5 Å of the N_ε atom of His-304. Thus, the water is in a suitable "substrate" position for a redox reaction of a dehydrogenase. There appears to be

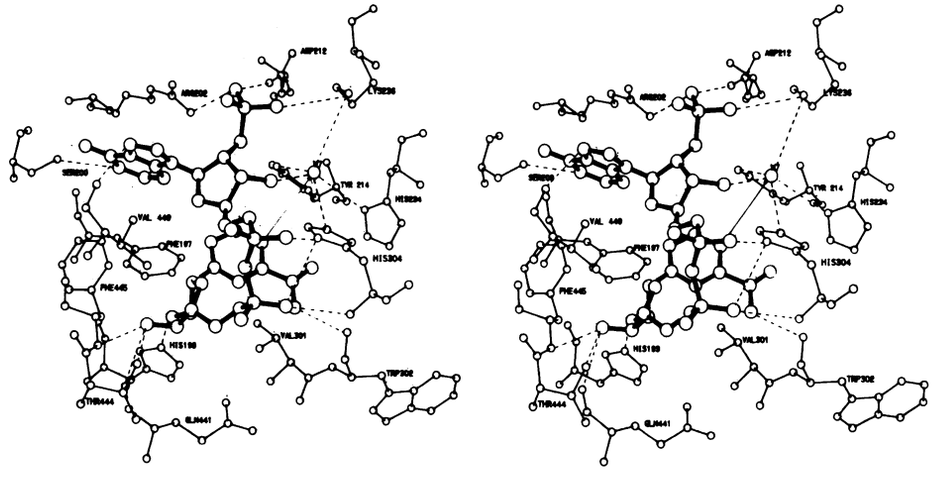

FIG. 4. Stereo view of NADP environment, showing hydrogen bonding and position of the W7 water molecule.

Table 4. NADP environment in BLC

NADP moiety	BLC residue	Interaction	Distance, Å; comment
Adenine	Ser-200	O_γ–N6A	2.9
	Phe-197		
	Arg-202	Aliphatic chain	Hydrophobic binding area
	Phe-445		
	Val-449		
Adenine ribose	Arg-202	$N_{\eta 2}$–OP2	2.7
	Lys-236	N_ε–OP3	3.5
Pyro-phosphate	His-304	N_δ–OP2A	2.9
	His-304	N–OP2N	3.0
	His-304	N_δ–OP2N	3.5
Nicotinamide ribose	His-193	N_ε–O2'N	2.6
	Gln-441	O–O3'N	2.8
	Thr-444	O_γ–O3'N	3.6
	Phe-197		
	Val-301		Hydrophobic pocket
	Phe-445		
	Val-449		
Nicotinamide	Val-301	C_β–N7N	3.2
	Trp-302	O–N7N	2.9
	His-304	C_ε–C4N	4.0
"Substrate" water (W7)	Tyr-214	O_η–W7	2.8
	Lys-236	N_ε–W7	4.4
	His-304	N_ε–W7	3.5
	Adenine ribose	O3'A–W7	2.9
	Nicotin-amide	C4N–W7	3.8

some feedback control on its binding, since the His-304 interacts both with this water substrate and the phosphates.

There is no direct interaction of the heme group and NADP. The closest approach of these two moieties is 13.7 Å between atoms C4N on NADP and the vinyl methyl group of pyrrole II of the heme group. The heme iron atom is 19.5 Å from the C4 atom of the nicotinamide ring. The β-sheet of the β-barrel domain lies between these two prosthetic groups and, in particular, the polypeptide β4 is interposed. It is noteworthy that the essential Asn-147 is situated on β4. The β-barrel domain of catalase consists of two halves. Each has four consecutive antiparallel β-sheets, β1, β2, β3, and β4 and β5, β6, β7, and β8. The binding of the heme group is effected primarily through residues on the β1–β4 section together with the "essential helix" α9 in the wrapping domain. The NADP molecule is bound primarily by residues in the β5–β8 barrel section (including α5) together with helix α10 in the α-helical domain.

There is no evidence for bound NADP in fungal catalases as observed by binding experiments to *Aspergillus niger* (1) or in the electron density map of PVC. Indeed, the BLC·NADP site is occupied by the hinge polypeptide in PVC (Table 1). The presence of the additional flavodoxin-like (α/β structure) domain in PVC might suggest that its function is similar to the NADP-binding function in BLC. Yet the position of the presumed FMN in PVC would be different from that of the NADP site observed in BLC (unpublished results). Furthermore, the α/β structures would select an extended FMN formation rather than the folded NADP structure found on BLC.

Conclusions

The site and conformation of NADP bound to BLC have been clearly established. Its relative closeness to the heme pocket suggests a relationship to the catalase activity, although no obvious function can be suggested. The folded conformation of the NADP is quite unlike the extended conformations found in numerous other structures. Its site closer to the carboxyl end of α-helices (with the phosphates furthest from the helix ends) is the converse to the well-characterized situation in many dehydrogenases or reductases. The position of a water molecule near the C4 carbon atom of the nicotinamide and its relationship to His-304 suggest a redox function.

We thank Dr. H. N. Kirkman for bringing his results to our attention prior to publication and for comments on this manuscript and Drs. B. Vainshtein and W. Melik-Adamyan for permission to view their electron density of *P. vitale* catalase in search of a possible bound NADP molecule. We also thank Sharon Wilder for help in the preparation of this manuscript. The work was supported by Grant PCM82-07747 from the National Science Foundation.

1. Kirkman, H. N. & Gaetani, G. F. (1984) *Proc. Natl. Acad. Sci. USA* **81**, 4343–4348.
2. Reid, T. J., III, Murthy, M. R. N., Sicignano, A., Tanaka, N., Musick, W. D. L. & Rossmann, M. G. (1981) *Proc. Natl. Acad. Sci. USA* **78**, 4767–4771.
3. Murthy, M. R. N., Reid, T. J., III, Sicignano, A., Tanaka, N. & Rossmann, M. G. (1981) *J. Mol. Biol.* **152**, 465–499.
4. Vainshtein, B. K., Melik-Adamyan, W. R., Barynin, V. V., Vagin, A. A. & Grebenko, A. I. (1981) *Nature (London)* **293**, 411–412.
5. Schroeder, W. A., Shelton, J. R., Shelton, J. B., Robberson, B., Apell, G., Fang, R. S. & Bonaventura, J. (1982) *Arch. Biochem. Biophys.* **214**, 397–421.
6. Catterall, W. A., Hollis, D. P. & Walter, C. F. (1969) *Biochemistry* **8**, 4032–4036.
7. Blumenstein, M. & Raftery, M. A. (1973) *Biochemistry* **12**, 3585–3590.
8. Saenger, W., Reddy, B. S., Mühlegger, K. & Weimann, G. (1977) in *Pyridine Nucleotide-Dependent Dehydrogenases*, ed. Sund, H. (de Gruyter, Berlin), pp. 222–236.
9. Chandrasekhar, K., McPherson, A., Jr., Adams, M. J. & Rossmann, M. G. (1973) *J. Mol. Biol.* **76**, 503–518.
10. Grau, U. M., Trommer, W. E. & Rossmann, M. G. (1981) *J. Mol. Biol.* **151**, 289–307.
11. Abdallah, M. A., Biellmann, J. F., Nordström, B. & Brändén, C. I. (1975) *Eur. J. Biochem.* **50**, 475–481.
12. Cedergren-Zeppezauer, E., Samama, J. P. & Eklund, H. (1982) *Biochemistry* **21**, 4895–4908.
13. Webb, L. E., Hill, E. J. & Banaszak, L. J. (1973) *Biochemistry* **12**, 5101–5109.
14. Moras, D., Olsen, K. W., Sabesan, M. N., Buehner, M., Ford, G. C. & Rossmann, M. G. (1975) *J. Biol. Chem.* **250**, 9137–9162.
15. Biesecker, G., Harris, J. I., Thierry, J. C., Walker, J. E. & Wonacott, A. J. (1977) *Nature (London)* **266**, 328–333.
16. Holden, H. M. & Banaszak, L. J. (1983) *J. Biol. Chem.* **258**, 2383–2389.
17. Stura, E. A., Zanotti, G., Babu, Y. S., Sansom, M. S. P., Stuart, D. I., Wilson, K. S., Johnson, L. N. & Van de Werve, G. (1983) *J. Mol. Biol.* **170**, 529–565.
18. Gronenborn, A. M., Clore, G. M. & Jeffery, J. (1984) *J. Mol. Biol.* **172**, 559–572.
19. Filman, D. J., Bolin, J. T., Matthews, D. A. & Kraut, J. (1982) *J. Biol. Chem.* **257**, 13663–13672.
20. Thieme, R., Pai, E. F., Schirmer, R. H. & Schulz, G. E. (1981) *J. Mol. Biol.* **152**, 763–782.
21. Wierenga, R. K., de Jong, R. J., Kalk, K. H., Hol, W. G. J. & Drenth, J. (1979) *J. Mol. Biol.* **131**, 55–73.
22. Wierenga, R. K., Drenth, J. & Schulz, G. E. (1983) *J. Mol. Biol.* **167**, 725–739.
23. Adams, M. J., Archibald, I. G., Bugg, C. E., Carne, A., Gover, S., Helliwell, J. R., Pickersgill, R. W. & White, S. W. (1983) *EMBO J.* **2**, 1009–1014.
24. Abdallah, M. A., Adams, M. J., Archibald, I. G., Biellmann, J. F., Helliwell, J. R. & Jenkins, S. E. (1979) *Eur. J. Biochem.* **98**, 121–130.
25. Schulz, G. E., Schirmer, R. H. & Pai, E. F. (1982) *J. Mol. Biol.* **160**, 287–308.
26. Hofsteenge, J., Vereijken, J. M., Weijer, W. J., Beintema, J. J., Wierenga, R. K. & Drenth, J. (1980) *Eur. J. Biochem.* **113**, 141–150.
27. Rossmann, M. G., Liljas, A., Brändén, C. I. & Banaszak, L. J. (1975) in *The Enzymes*, ed. Boyer, P. D. (Academic, New York), 3rd Ed., Vol. 11, pp. 61–102.
28. Reddy, B. S., Saenger, W., Mühlegger, K. & Weimann, G. (1981) *J. Am. Chem. Soc.* **103**, 907–914.
29. Parthasarathy, R. & Fridey, S. M. (1984) *Science* **226**, 969–971.
30. Hol, W. G. J., van Duijnen, P. T. & Berendsen, H. J. C. (1978) *Nature (London)* **273**, 443–446.
31. Rossmann, M. G., Moras, D. & Olsen, K. W. (1974) *Nature (London)* **250**, 194–199.
32. Ohlsson, I., Nordström, B. & Brändén, C. I. (1974) *J. Mol. Biol.* **89**, 339–354.
33. Rao, S. T. & Rossmann, M. G. (1973) *J. Mol. Biol.* **76**, 241–256.
34. Arnott, S. & Hukins, D. W. L. (1969) *Nature (London)* **224**, 886–888.
35. Wright, W. B. & King, G. S. D. (1954) *Acta Crystallogr.* **7**, 283–288.